



Published in final edited form as:

*Endocrinology*. 2005 March ; 146(3): 1245–1253.

## Preservation of Eumelanin Hair Pigmentation in Proopiomelanocortin-Deficient Mice on a Nonagouti (*a/a*) Genetic Background

Andrzej Slominski, Przemyslaw M. Plonka, Alexander Pisarchik, James L. Smart, Virginie Tolle, Jacobo Wortsman, and Malcolm J. Low

Department of Pathology and Laboratory Medicine (A.S., A.P.), University of Tennessee, Memphis, Tennessee 38163; Department of Biophysics (P.M.P.), Faculty of Biotechnology, Jagiellonian University, 30-387 Krakow, Poland; Vollum Institute (J.L.S., V.T., M.J.L.), Department of Behavioral Neuroscience (M.J.L.), and Center for the Study of Weight Regulation and Associated Disorders (M.J.L.), Oregon Health and Science University, Portland, Oregon 97239; and Department of Medicine (J.W.), Southern Illinois University, Springfield, Illinois 62704

### Abstract

The original strain of proopiomelanocortin (POMC)-deficient mice (*Pomc*<sup>-/-</sup>) was generated by homologous recombination in 129X1/SvJ (*A<sup>w</sup>/A<sup>w</sup>*)-derived embryonic stem cells using a targeting construct that deleted exon 3, encoding all the known functional POMC-derived peptides including  $\alpha$ MSH, from the *Pomc* gene. Although these *Pomc*<sup>-/-</sup> mice exhibited adrenal hypoplasia and obesity similar to the syndrome of POMC deficiency in children, their agouti coat color was only subtly altered. To further investigate the mechanism of hair pigmentation in the absence of POMC peptides, we studied wild-type (*Pomc*<sup>+/+</sup>), heterozygous (*Pomc*<sup>+/-</sup>), and homozygous (*Pomc*<sup>-/-</sup>) mice on a nonagouti (*a/a*) 129;B6 hybrid genetic background. All three genotypes had similar black fur pigmentation with yellow hairs behind the ears, around the nipples, and in the perianal area characteristic of inbred C57BL/6 mice. Histologic and electron paramagnetic resonance spectrometry examination demonstrated that hair follicles in back skin of *Pomc*<sup>-/-</sup> mice developed with normal structure and eumelanin pigmentation; corresponding molecular analyses, however, excluded local production of  $\alpha$ MSH and ACTH because neither *Pomc* nor putative *Pomc* pseudogene mRNAs were detected in the skin. Thus, 129;B6 *Pomc* null mutant mice produce abundant eumelanin hair pigmentation despite their congenital absence of melanocortin ligands. These results suggest that either the mouse melanocortin receptor 1 has sufficient basal activity to trigger and sustain eumelanogenesis *in vivo* or that redundant nonmelanocortin pathway(s) compensate for the melanocortin deficiency. Whereas the latter implies feedback control of melanogenesis, it is also possible that the two mechanisms operate jointly in hair follicles.

---

Address all correspondence and requests for reprints to: Malcolm J. Low, M.D., Ph.D., Vollum Institute, L-474, Oregon Health and Science University, 3181 SW Sam Jackson Park Road, Portland, Oregon 97239-3098. E-mail: low@ohsu.edu..

This work was supported by National Institutes of Health Grants DK66604 (to M.J.L.), HG00201 (to J.L.S.) and AR47079 (to A.S.) and grants from the Center of Excellence in Genomics and Bioinformatics and the Center of Excellence in Connective Tissue Diseases, University of Tennessee Health Science Center (to A.S.) and the Center of Excellence in Molecular Biotechnology founded by the European Union and the Polish Ministry of Science and Information (project BIER, contract no. ICA1-CT-2000-70012 and SPUB-M 3018, Workpackage 6) (to P.M.P.). V.T. was the recipient of an American Society for Pharmacology and Experimental Therapeutics/Merck postdoctoral fellowship in integrative pharmacology.

## Abbreviations

AGP, Agouti protein; DPPH, 1,1-diphenyl-2-picrylhydrazyl; EPR, electron paramagnetic resonance; GAPDH, glyceraldehyde-3-phosphate dehydrogenase; L-DOPA, L-dihydroxyphenylalanine; MC1-R, melanocortin receptor type 1; POMC, proopiomelanocortin; RT, reverse transcription

Melanin Biosynthesis is initiated both *in vivo* from the obligatory hydroxylation of *in vitro* and L-tyrosine to L-dihydroxyphenylalanine (L-DOPA), catalyzed by tyrosinase (EC 1.14.18.1) (1–3). Once L-DOPA is formed, further steps of melanogenesis consisting of a series of oxidoreduction reactions and intramolecular transformations can occur spontaneously and at varying rates, depending on local concentrations of hydrogen ions, metal cations, reducing agents, thiols, and oxygen (1). Eumelanogenesis involves the transformation of dopaquinone to leukodopachrome, followed by a series of oxidoreduction reactions with production of the intermediates dihydroxyindole and dihydroxyindole carboxylic acid, which undergo polymerization to form eumelanin (1,4,5). Pheomelanogenesis also starts with dopaquinone, which is conjugated to cysteine or glutathione to yield cysteinyl-dopa and glutathionyl-dopa for further transformation into pheomelanin (1,5,6).

Although tyrosinase activity is the rate-limiting step among the melanogenesis-related enzymes (1,7,8), pigmentation is under complex genetic control regulated by more than 150 alleles representing more than 90 gene loci (3,9–14). Protein products of these loci include enzymes, structural proteins, transcriptional regulators, transporters, receptors, and growth factors with a wide array of functions and cellular targets (3,13). Among them are the important structural, enzymatic and regulatory proteins coded by *albino(c)/TYR*, *brown(b)/TYRP1*, *slaty (slt)/TYRP2/DCT*, *silver(slt)/SILV*, *pink-eyed dilute(p)/P/OCA2*, *under-white(uw)/LOC51151*, *MART1*, *OAI* loci, *melanocortin receptor type 1 (MC1-R)*, *proopiomelanocortin (POMC)*, and *agouti (AGP)* (3,13).

The melanogenic effects of POMC-derived MSH and ACTH peptides have been documented in a number of vertebrate species (3,13,15,16). Thus, in amphibians  $\alpha$ - and  $\beta$ MSH induce darkening of the skin (reviewed in Ref. 16), whereas in mammalian systems such as rodents, MSH peptides stimulate both melanogenesis and the switch from pheo- (yellow/red) to eumelanogenic (black) pathways (13,17–22). In humans the systemic administration of  $\alpha$ MSH,  $\beta$ MSH, or ACTH stimulates skin pigmentation, predominantly in sun-exposed areas, whereas pathologically increased plasma ACTH levels (Addison's disease or Nelson's syndrome) induce hyperpigmentation and skin atrophy (15). Conversely, patients with *POMC* gene mutations leading to defective production of the POMC prohormone in all tissues show a red hair phenotype in addition to early-onset obesity and adrenal insufficiency (23). Recessive mutations in the MC1-R that produce unresponsiveness of epidermal melanocytes to  $\alpha$ MSH also result in the red hair phenotype (13,24) in humans or yellow fur in mice, whereas a dominant allele produces a constitutively active MC1-R that results in uniform jet black fur in somber mice (25).

Agouti coloration in wild-type mice is characterized by a banded pigmentation pattern of the pelage, in which each hair is black with a subapical band of yellow. AGP (the product of *agouti* locus A) is produced in dermal papilla cells and acts within the microenvironment of the hair follicle during hair growth to transiently switch eumelanin synthesis into pheomelanin synthesis, thereby generating the agouti coat color (12,26–28). Several studies have demonstrated that AGP can function as a competitive antagonist of the MC1-R, blocking its activation by  $\alpha$ MSH (3,13,26) or as an inverse agonist (29,30). AGP therefore suppresses melanogenesis by decreasing tyrosinase activity, decreasing expression of melanogenic genes

including those that encode tyrosinase and tyrosinase-related protein 1 and 2 and inhibiting translation of MC1-R (3,13,31).

Melanocortin and ACTH sequences are encoded within exon 3 of the *Pomc* gene (32), which in addition to the pituitary, is transcribed, translated, and processed in the central nervous system (33) and a variety of peripheral tissues including skin (15). Concordantly, two distinct strains of *Pomc*-null mice generated independently on either a hybrid 129X1;129S6 genetic background (34) or a 129S6;129S2 genetic background (35) exhibit a syndrome of adrenal insufficiency, obesity, and a subtle alteration in coat color distinguished by a lighter yellow tint to agouti-banded hairs that is most pronounced on their bellies. However, when the null *Pomc* allele was backcrossed from the 129X1;129S6 white-bellied agouti genetic background ( $A^w/A^w$ ) onto the C57BL/6J non-agouti ( $a/a$ ), genetic background for two generations the *Pomc*<sup>-/-</sup> offspring exhibited black fur pigmentation visually indistinguishable from sibling controls expressing the wild-type *Pomc* allele (36). This persistence of black pigmentation contrasts with the red hair phenotype of human POMC deficiency (23). It is also at variance with our own observations in the C57BL/6 mouse strain of anagen coupling to melanogenesis and enhanced cutaneous expression of the *Pomc* and *Mclr* genes (15,37,38). Therefore, we performed detailed histological studies of skin and hair follicle structure with biophysical analyses of the pigment type produced in *Pomc*<sup>-/-</sup> mice. The results were then correlated with molecular analyses of local POMC expression.

## Materials and Methods

### Animals

The mutant *Pomc* allele designed to delete exon 3 of the gene, which encodes all the known functional peptides, was originally constructed and targeted into strain 129X1/SvJ ( $A^w/A^w$   $pTyr^{c-ch}/pTyr^c$ )-derived RW-4 embryonic stem cells by Yaswen *et al.* (34) and then subsequently carried on a hybrid 129X1;129S6 genetic background ( $A^w/A^w$  +/?). After two sequential generations of backcrossing the mutant *Pomc* allele onto the C57BL/6J ( $a/a^{+/+}$ ) background (The Jackson Laboratory, Bar Harbor, ME), a colony of hybrid 129;B6 mice (approximately 75% of alleles from B6) was established in Portland, and all experimental animals were derived from heterozygous breeding pairs of mice with genotypes ( $Pomc^{+/-}a/a^{+/+}$ ). Mice were genotyped at the *Pomc* locus by PCR using two oligonucleotide primer pairs: 5'-GCTTGCATCCGGGCTTG-CAAAC-3' and 5'-AGCAACGTTGGGGTACACCTTC-3' amplify a 318-bp wild-type allele; 5'-TTGTTAACTTGTTTATTGCAGCTT-3' and 318-bp 5'-ATGAGAAATTGGGCCATGGGACTGAC-3' amplify an approximately 300-bp mutant allele. All procedures with mice followed the recommendations in the National Institutes of Health Public Health Service Guide for the Care and Use of Laboratory Animals and were approved by the Institutional Animal Care and Use Committee at Oregon Health and Science University.

### Tissue processing

Murine tissue samples consisted of skin isolated at telogen and anagen (d 5 to 7 post depilation) stages of the hair cycle. The animals (9 month old male mice) were euthanized under 2% Avertin (2,2,2-tribromo-ethanol) anesthesia, and back skin was collected following protocols routinely used in our laboratory. Tissue specimens were either frozen rapidly in liquid nitrogen and stored at -80 C until further analysis or fixed in 10% buffered formalin, paraffin embedded, and stained with hematoxylin and eosin (38).

### Preparation of samples for electron paramagnetic resonance (EPR) assay

Fur was obtained from the back of anesthetized adult mice using an electric clipper, collected into individual preweighed polypropylene tubes, and stored dry at room temperature until

analysis. We compared fur of test mice (either *Pomc*<sup>-/-</sup> or *Pomc*<sup>+/+</sup>) with fur of standard black C57BL/6J mice containing eumelanin and with samples of yellow fur containing pheomelanin, *i.e.* C57BL/6J *A<sup>Y</sup>/a* mice (39,40), and the yellow form of Mongolian gerbil (*Meriones unguiculatus*) (41). We also compared the EPR signals of fur with the signals of synthetic melanins.

Dopa-melanin, the synthetic counterpart of eumelanin, was synthesized by dopa autooxidation (42). The aqueous solution of D,L-dopa was bubbled with air for 4 d at ambient temperature, whereas the pH was kept constant at 8.0 (NH<sub>4</sub>OH). The synthetic equivalent for a natural pheomelanin was prepared by enzymatic oxidation of L-DOPA and L-cysteine (according to Ref. 43). The solution of 994 mg L-DOPA and a double excess of L-cysteine (448 mg) in 500 ml Sorensen's buffer [Na<sub>2</sub>HPO<sub>4</sub>/KH<sub>2</sub>PO<sub>4</sub>, 0.01 M (pH 6.8)] was supplemented with 200,000 U of yeast tyrosinase in 25 ml of the same buffer, stirred for 1 h, and bubbled for 4 d with air. Both melanins were then precipitated from solution by lowering the pH to 3.0–3.5 with concentrated HCl, purified with several washings with redistilled water, and dialyzed against re-distilled water for 4 d. The substances were then dried for 4 d in the air at 37 C and introduced into glass capillaries that were sealed by melting and solidifying their ends. Every sample contained 8.2 ± 0.1 mg of dry powdered melanin. All the reagents were obtained from Sigma Chemical Co. (St. Louis, MO).

### EPR spectrometry

All the measurements were carried out at room temperature using a Varian 103 EPR X-band spectrometer (Varian, Inc., Palo Alto, CA) with 100 kHz modulation frequency and a rectangular TE 102 resonant cavity. Samples of fur (20 ± 1 mg) and capillaries with melanins were put into a quartz finger Dewar and then always placed in the cavity in the same position against the modulation field. Parameters of measurements were as follows: magnetic field 3265 ± 50 Gs; modulation amplitude 5 Gs for quantitative comparisons; 2 Gs to record the signal shape; and 0.5 Gs to measure the signal peak-to-peak width, microwave frequency 9.17 GHz, and power 1 mW. Spectra were acquired in a digital form (1024 points per scan) at 0.1 or 0.3 time constant, 90–180 time scan, 1–7 times (averaged), at instrumental gain 12,500 to 1 million according to the particular signal to noise ratio. All the signal intensities were expressed as integral intensities (by double integration of signal curves), whereupon means ± SEM of at least five independent samples were calculated to prepare bar plots. The quantitative data were additionally recalculated for a constant gain (12,500) and constant sample mass (20 mg). All the conclusions drawn from the comparisons of the integral intensities were additionally confirmed by comparing peak-to-peak amplitudes of the signals. A small powder sample of 1,1-diphenyl-2-picrylhydrazyl (DPPH) served as a marker for the position of the free radical signal (*g* = 2.0037). The statistical significance of the differences in signal intensities and widths were tested by the independent two-tailed Student *t* test and accepted for *P* < 0.05.

### cDNA preparation

Total RNA was extracted using a Trizol isolation kit (Life Technologies, Inc.-BRL, Gaithersburg, MD), whereas poly (A<sup>+</sup>) mRNA was isolated using Oligotex mRNA minikit (Qiagen, Valencia, CA). RNA samples were treated with DNase before reverse transcription (RT), and only those samples that were negative for glyceraldehyde-3-phosphate dehydrogenase (GAPDH) genomic sequences by PCR amplification were used for RT (44). The synthesis of first-strand cDNA was performed using the Superscript preamplification system (Invitrogen, Carlsbad, CA). An aliquot of 5 µg total RNA or 0.1 µg mRNA per reaction was reverse transcribed using oligo(dT) as the primer. The expression of genes having only one coding exon was evaluated using cDNA synthesized from DNase-treated RNA. Lack of DNA contamination was confirmed by negative amplification of RNA without prior RT.

## PCRs

All primers were synthesized by Integrated DNA Technology Inc. (Coralville, IA). All samples were standardized by the amplification of the housekeeping gene GAPDH as described previously (44).

Detection of mouse *Pomc* and *Pomc-ps1* pseudogene was obtained by direct or nested PCR amplifications of the corresponding cDNAs. Sequences of the primers used for PCR amplifications are listed in Table 1, whereas their exon location together with gene structure is presented in Fig. 1. The reaction mixture (25  $\mu$ l) contained 3.0 mM MgCl<sub>2</sub>, 0.25 mM of each deoxynucleotide triphosphate, 0.4  $\mu$ M of each primer, 75 mM Tris-HCl (pH 8.8), 20 mM (NH<sub>4</sub>)<sub>2</sub>SO<sub>4</sub>, 0.01% Tween 20, and 1.25 U of Taq polymerase (Promega, Madison, WI). The mixture was heated to 95 C for 3 min and then amplified for 35 cycles as specified: 94 C for 30 sec (denaturation), 55 C for 30 sec (annealing), and 72 C for 40 sec (extension). Amplification products were separated by agarose gel electrophoresis and visualized by ethidium bromide staining according to standard protocols used in our laboratory (44). For nested PCR the mixtures were amplified for 25 cycles as described above during the first round of amplification. Five microliters were used for a second cycle of amplification using primers described in Table 1 and the program described above.

## Sequencing

The identified PCR products were excised from the agarose gel and purified by GFX PCR DNA and gel band purification kit (Amersham Pharmacia Biotech, Piscataway, NJ). PCR fragments were cloned in pGEM-Teasy vector according to the protocol of the manufacturer (Pro-mega). Plasmid DNA was purified by a plasmid minikit (Qiagen). Sequencing was performed in the Molecular Resource Center at the University of Tennessee Health Science Center (Memphis) using the 3100 genetic analyzer (Applied Biosystems, Foster City, CA) and BigDye terminator kit.

## Results

The *Pomc*<sup>-/-</sup> mutant mice described by Yaswen *et al.* (34) were generated originally on a hybrid 129X1;129S6 genetic background (*A<sup>w</sup>/A<sup>w</sup>/?*). Therefore, these mice were homozygous for the white-bellied agouti allele (*A<sup>w</sup>/A<sup>w</sup>*) and either homozygous for the wild-type *Tyrosinase* allele (+/+) or heterozygous for one of the recessive *Tyrosinase* alleles pink-eyed chinchilla (+/*pTyr<sup>c-ch</sup>*) or pink-eyed albino (+/*pTyr<sup>c</sup>*) present in the genome of the RW4 embryonic stem cells that were used for POMC gene targeting by homologous recombination. We further evaluated the contribution of the *Pomc*<sup>-/-</sup> genotype to hair follicle pigmentation after back-crossing the null *Pomc* allele for two generations onto the nonagouti C57BL/6J (*a/a<sup>+/+</sup>*) genetic background.

All N<sub>1</sub> heterozygous 129;B6 (*Pomc*<sup>+/-</sup> *A<sup>w</sup>/a<sup>+/?</sup>*) mice had fur pigmentation characteristic for expression of the dominant *A<sup>w</sup>* and wild-type *Tyrosinase* alleles: dark agouti hairs on the back and lighter white/yellow hairs on the belly. In contrast, one fourth of the N<sub>2</sub> heterozygous *Pomc* mice had black fur consistent with a (*Pomc*<sup>+/-</sup> *a/a<sup>+/?</sup>*) genotype and the remaining three fourths all had coat coloring identical with the agouti N<sub>1</sub> generation mice. Intercrossing of black N<sub>2</sub> heterozygous *Pomc* mice yielded offspring with each of the three possible *Pomc* genotypes, all of which had indistinguishable black fur pigmentation with scattered yellow hairs behind the ears on the ventral surface of the neck, around the nipples, and in the perianal area (Fig. 2, A–H). No mice with pink eyes and chinchilla or albino fur have been found of a total population of more than 500 born to multiple N<sub>2</sub> heterozygous *Pomc* breeder pairs, indicating with virtual certainty that the recessive *pTyr<sup>c-ch</sup>* and *pTyr<sup>c</sup>* alleles were eliminated from our breeding colony by segregation at an earlier generation and therefore that all the mice

studied must be homozygous for the wild-type *Tyrosinase* allele. The same phenotype of uniformly black fur was observed after synchronous anagen induction by hair depilation in *Pomc*<sup>+/+</sup> and *Pomc*<sup>-/-</sup> mice (Fig. 2, I and J).

Morphological examination showed almost identical histoarchitecture in skin from *Pomc*<sup>-/-</sup> and *Pomc*<sup>+/+</sup> mice at telogen and anagen phases of hair growth mice (Fig. 3, A-D). Thus, the epidermis and dermis with its adnexal structures had the same characteristic features as those described previously in the control C57BL/6J mice (38). Furthermore, *Pomc*<sup>-/-</sup> mice showed normally developing anagen hair follicles with identical structure to that observed in *Pomc*<sup>+/+</sup> and C57BL/6J control mice (Fig. 3, E and F, *left panels*). The hair follicles were melanogenically active producing black hair shafts with a characteristic banding (Fig. 3, E and F, *right inset panels*).

Hair shafts obtained from *Pomc*<sup>-/-</sup> mice, as well as from *Pomc*<sup>+/+</sup> and C57BL/6J (*a/a*) mice, were all homogeneously black and revealed a slightly asymmetric singlet EPR signal placed around  $g = 2.0037$  (Fig. 4). This singlet corresponded to a DPPH-free radical standard and had a similar shape as the signal of synthetic dopa melanin (Fig. 4). The hair samples also revealed very similar widths of the EPR lines, approximately 0.5 Gs higher than the synthetic dopa melanin signals (4.7 Gs vs. 4.2 Gs). The other materials analyzed in this study, *i.e.* synthetic cysteinyl-dopa melanin, fur of C57BL/6J (*A<sup>y</sup>/a*), and fur of yellow gerbils, exhibited EPR signals with clear hyperfine structure connected to the location of unpaired electrons near the nucleus of <sup>14</sup>N (41,45,46). These pheomelanin-containing materials also revealed much wider EPR signals (approximately 6–7 Gs), compared with black fur and synthetic dopa melanin (Fig. 5B  $P < 10^{-3}$  to  $P < 10^{-5}$ ). Quantitative analyses of eumelanin were also performed (Fig. 5A). As expected, the EPR signal intensity was lower by at least of 1 order of magnitude ( $P < 10^{-3}$  to  $P < 10^{-6}$ ) in furs of obese yellow *A<sup>y</sup>/a* mice and yellow gerbils, which produced pheomelanin, than the black furs. The synthetic cysteinyl-dopa melanin revealed an approximately 50% lower EPR signal than dopa melanin (Fig. 5A). Interestingly, the genetically manipulated 129;B6 mice tended to have lower eumelanin content than pure C57BL/6J (Fig. 5), but there was no statistically significant difference between the hybrid 129;B6 *Pomc*<sup>-/-</sup> and C57BL/6J mice.

The presence of a hyperfine structure of the EPR signal of pigments containing a contribution of pheomelanin originates from the difference in the chemical character of pheomelanin-like paramagnetic centers being of a semiquinonimine rather than semiquinone character (43) and is considered a *sine qua non* for the presence of pheomelanin in biological samples (47). Conversely, the lack of this structure in a signal strongly suggests the lack of pheomelanin in an investigated material but does not represent an absolute proof because trace amounts of pheomelanin might be effectively masked by a strong eumelanin-like signal. Nevertheless, other differences in the signal satisfactorily supplement the notion that the *Pomc* null mutation did not result in any substantial pheomelanogenesis in our model because the black furs differed only slightly in their EPR signal intensity (Fig. 5A) but not in their peak-to-peak widths (Fig. 5B). In contrast, the pheomelanin-containing furs always revealed an EPR signal of at least 1 order of magnitude lower intensity, consistent with other studies on the chemical method of pheomelanin estimation (39,40). The higher values of the signal peak-to-peak width of natural pigments in comparison with their synthetic counterparts (Fig. 5B) is not surprising due to the constitutive presence of some amounts of paramagnetic metal ions (iron, copper, manganese) in natural melanins (48). However, the pheomelanin-like signals are always wider than the ones of eumelanins (45) (see cysteinyl-dopa vs. dopa melanin or pheomelanin-containing fur vs. black fur signals in Fig. 5B). Judging by the line width and the lack of hyperfine structure, all the pigments of the investigated black furs, including *Pomc*<sup>-/-</sup> and C57BL/6J-derived hair shafts, revealed EPR signals of very similar shapes, betraying a prominent homogeneity of the population of corresponding paramagnetic centers. If the *Pomc*<sup>-/-</sup> mice or wild-type

*Pomc*<sup>+/+</sup> mice contain any traces of pheomelanin that cannot be detected by EPR, their contribution to the resulting paramagnetism of pigments would be no bigger than that in the eumelanin-containing C57BL/6J mice.

To test for the possibility of residual local production of  $\alpha$ MSH and ACTH in the *Pomc*<sup>-/-</sup> mice, we performed molecular analyses for *Pomc* gene expression in back skin (Fig. 6). Neither direct nor nested RT-PCR with primers at exons 2 vs. 3 or solely at exon 3 could detect POMC mRNA in back skin from 129;B6 *Pomc*<sup>-/-</sup> mice (Fig. 6). Predictably, POMC mRNA was detected in the skin of sibling control 129;B6 *Pomc*<sup>+/+</sup> and *Pomc*<sup>-/-</sup> mice. Sequencing of the PCR-amplified DNA products from the latter mice confirmed their identity as transcripts from the *Pomc* gene (data not shown). As a further control, POMC mRNA was also detected in the skin of mice generated by crossing a 10-kb *Pomc* transgene containing 2 kb of promoter sequences and the intact transcriptional unit (Smart, J. L., V. S. Tolle, and M. J. Low, manuscript in preparation) onto the *Pomc*<sup>-/-</sup> background. The 10-kb transgene contains regulatory elements that rescue transcription of *Pomc* to skin structures as well as pituitary cells of the compound mutant mice. Lastly, we also tested possible transcription of the *Pomc-ps1* pseudogene using RT-PCR with the expected negative results (Fig. 7).

## Discussion

We have demonstrated that nonagouti 129;B6 POMC-deficient mice are skin negative for mRNA corresponding to either the *Pomc* or *Pomc-ps1* genes, but their hair follicle development, structure, and melanin pigmentation are similar to control 129;B6 *Pomc*<sup>+/+</sup> and inbred wild-type C57BL/6J mice. Therefore, 129;B6 *Pomc*<sup>-/-</sup> mice can produce eumelanin hair pigmentation despite a total absence of local and systemic  $\alpha$ MSH or ACTH ligands.

These findings are significant because  $\alpha$ MSH and ACTH are recognized as major regulators of melanin pigmentation in rodents and humans (13,15,16). Melanocortin peptide effects are mediated through a signal cascade that includes ligand interactions with the stimulatory G protein-coupled MC1-R, activation of cAMP-dependent pathways, and stimulation or induction of eumelanogenesis (13,15,49). The eumelanogenic pathway is counteracted by AGP, both a functional antagonist of melanocortins and an inverse agonist at MC1-R, which inhibits expression and activity of melanogenesis-related proteins, melanogenic enzymes, and MC1-R, thereby inducing the switch from eu- to pheomelanogenesis (3,26,27,31). It is important to note that the switch between pheo- to eumelanogenesis in normal agouti fur is of a discontinuous on or off character-pheomelanin usually produced in low amounts at low levels of tyrosinase activity, whereas pure eumelanin is generated over a threshold value of tyrosinase activity (50). Eumelanosomes also differ in structure and shape from pheomelanosomes (1,3, 51). It is therefore highly unlikely that low amounts of pheomelanin in the absence of AGP expression are generated in parallel to the ongoing eumelanogenesis in the same melanosome and at the same time. If the quality of melanogenesis was changed due to the deletion of POMC in our model, it should have resulted in a drastic reduction of the total amount of pigment, such that the presence of the EPR signal features attributed to pheomelanin would be detectable. In fact, the absence of POMC did not result in a qualitative change of melanogenesis, compared with the parental C57BL/6J mice as measured by EPR spectroscopy and morphologic and histological examinations.

It is probable that the eumelanogenic phenotype in the 129;B6 *Pomc*<sup>-/-</sup> mice is due to a relatively high basal (*i.e.* ligand-independent) activity of MC1-R based on the following considerations: 1) MC1-R can be stimulated to couple to G proteins and stimulate the production of intracellular cAMP independently from its peptide agonists, *i.e.* by metal ions (52); 2) basal activity of MC1-R increases directly with greater receptor number (in malignant melanocytes) (53); 3) MC1-R expression is hair cycle dependent with the highest expression

levels at anagen V-VI (when the melanogenic activity reaches its peak) and lowest at telogen (resting phase) (37); 4) MC1-R variants strongly correlate with the type and degree of melanin production throughout the animal kingdom (54); and 5) AGP (an intrinsic inhibitor of MC1-R activity) was absent or very low (12,26,27).

Therefore, the presumed event that prevents the switch from eu- to pheomelanogenesis in 129;B6 *Pomc*<sup>-/-</sup> mice is the lack or very low concentration of AGP dictated by the (*a/a*) genotype (12,26,27). In turn, this would allow maintenance of eumelanin synthesis through high basal ligand-independent or stimulated MC1-R activity (see above) and appears to be consistent with the hypothesis of a bimodal switch regulating the passage from eu- to pheomelanogenesis (50). Stimulatory signals could also be provided by factors acting at the postreceptor level (MC1-R-independent pathways), either by directly raising intracellular cAMP levels or by stimulating protein kinase A; intracellular second-messenger pathways critical for melanogenesis in rodents (49,55). This postulation of multiple regulatory points of melanogenesis, *i.e.* direct regulation through receptor mediated or metabolic action on melanocytes and indirect through stimulation of other cellular targets, which in turn release biologic regulators or simply change the chemical environment of melanocytes is consistent with current concepts of melanin production (51). The process is thought to be redundant and determined by multiple regulatory factors including a time-frame and spatial-temporal dependence on both feedback and feed-forward controls in place from embryonic to adult life (51). The heterogeneous and redundant nature of proeumelanogenic signals explains why the deletion of only one, but a very important, regulatory factor (the agonist ligands for the MC1-R) is not sufficient to produce a dramatic change of melanogenesis in a predominantly C57BL/6 genetic background.

Previously published studies indicated that mammalian MC1-Rs can exhibit agonist-independent, constitutive activity *in vitro*. One of the first reports (56) used the amelanotic mouse melanoma cell line B16-G4F stably transfected with the human MC1-R. More recently the human MC1-R was shown to constitutively activate cAMP production in transfected, heterologous human embryonic kidney 293T, HeLa, and Chinese hamster ovary cell lines in addition to overexpression in HBL human melanoma cell lines (57). Importantly, the latter study also demonstrated significant constitutive activity of the mouse MC1-R in transfected human embryonic kidney 293T cells. The intrinsic signaling activity of mouse MC1-R was lower than human MC1-R at similar binding site densities, but the two species exhibited comparable augmentation of forskolin-mediated cAMP production (57).

Many other G protein-coupled receptors demonstrate significant constitutive activity (58,59). Particularly relevant is the finding that both MC3-R and MC4-R have high levels of basal signaling revealed by the inverse agonist activity of agouti-gene-related protein (60). Similarly the endogenous cannabinoid receptors CB1 and CB2 (61,62), the angiotensin II receptor (63), and several classes of 5-hydroxytryptamine receptors are constitutively active (64,65). In other cases, such as the mu opioid receptor, prolonged agonist exposure appears to induce constitutive activity in the subsequent absence of ligand (66) and activating mutations can readily be introduced into this and many other G protein-coupled receptors. Notable examples of spontaneous mutations leading to clinical disorders from agonist-independent receptor activation include the TSH receptor associated with thyrotoxicosis (67) and the LH receptor leading to precocious puberty (68). Therefore, ample precedents support the concept of high basal activity of the MC1-R in the absence of melanocortin peptide stimulation.

Within the context of the above, the present findings do not contradict the previous concept of induction of a mild pheomelanin-like phenotype in homozygous *Pomc*<sup>-/-</sup> mice on a hybrid agouti 129 genetic background that was reverted by  $\alpha$ MSH treatment (34). Thus, genetic background represented, *i.e.* by the presence or absence of AGP, would take priority over the

regulatory role of MSH or ACTH in melanogenesis. This is consistent with the current concept proposing that melanogenesis-controlling factors are not arranged in simple linear sequences; instead they interact in a multidimensional network, with extensive overlapping and diversity of factors acting in a stochastic fashion determined by the genetic-biochemical-physical context (51).

In summary, we demonstrate that deletion of the *Pomc* gene in nonagouti 129;B6 mice does not significantly reduce total melanin production or induce a switch to pheomelanogenesis. We suggest that the phenotype results from ligand-independent activation of MC1-R, which triggers and sustains eumelanogenesis *in vivo*. This mechanism is consistent with published reports of constitutive MC1-R activity in transfected cell lines *in vitro*, often positively correlated with increased receptor density per cell, but does not necessarily imply a paramount role in melanogenesis under normal physiological conditions. Our data do not exclude the possibility that genetic deletion of melanocortin ligands has a stimulatory effect on MC1-R signaling by either increases in receptor number or intrinsic activity, and this in turn contributed to the lack of any change in fur pigmentation. Additionally, redundant nonmelanotropic pathway(s) may be recruited to ensure eumelanin pigmentation in the absence of both melanocortin peptides and AGP. One example of an alternative paracrine pathway could involve TRH, which has been demonstrated to bind and activate the MC1-R with low micromolar affinity and to be synthesized in hair follicle papilla fibroblasts (69,70). Overall, our findings serve to reinforce the conclusion, that despite the overwhelming dominance of POMC-derived peptides in the stimulation of melanogenesis, skin and hair pigmentation are complex, polygenic traits (51).

#### Acknowledgements

Breeder *Pomc*<sup>+/-</sup> mice on the 129X1;129S6 background were kindly provided by Dr. U. Hochgeschwender (Oklahoma Medical Research Foundation, Oklahoma City, OK).

#### References

1. **Prota G** 1992 Melanins and melanogenesis. New York: Academic Press
2. Korner A, Pawelek J. Mammalian tyrosinase catalyzes three reactions in the biosynthesis of melanin. *Science* 1982;217:1163–1165. [PubMed: 6810464]
3. Hearing VJ. Biochemical control of melanogenesis and melanosomal organization. *J Invest Dermatol Symp Proc* 1999;4:24–28.
4. Pawelek JM. After dopachrome? *Pigment Cell Res* 1991;4:53–62. [PubMed: 1946209]
5. Ito S. The IFPCS presidential lecture: a chemist's view of melanogenesis. *Pigment Cell Res* 2003;16:230–236. [PubMed: 12753395]
6. Prota G. The chemistry of melanins and melanogenesis. *Fortsch Chem Org Naturst* 1995;64:93–148.
7. Hearing VJ, Tsukamoto K. Enzymatic control of pigmentation in mammals. *FASEB J* 1991;5:2902–2909. [PubMed: 1752358]
8. Pawelek JM, Korner AM. The biosynthesis of mammalian melanin. *Am Sci* 1982;70:136–145. [PubMed: 7091866]
9. Hearing VJ. The melanosome: the perfect model for cellular responses to the environment. *Pigment Cell Res* 2000;13(Suppl 8):23–34. [PubMed: 11041354]
10. Jackson IJ. Molecular and developmental genetics of mouse coat color. *Annu Rev Genet* 1994;28:189–217. [PubMed: 7893123]
11. Schallreuter KU, Wood JM. The importance of l-phenylalanine transport and its autocrine turnover to l-tyrosine for melanogenesis in human epidermal melanocytes. *Biochem Biophys Res Commun* 1999;262:423–428. [PubMed: 10462491]
12. **Silvers W, ed** 1979 The coat colors of mice. A model for mammalian gene action and interaction. New York: Springer Verlag

13. Nordlund JJ, Boissy RE, Hearing VJ, King RA, Ortonne JP 1988 The pigmentary system. Physiology and pathophysiology. New York and Oxford: Oxford University Press
14. Kushimoto T, Valencia JC, Costin GE, Toyofuku K, Watabe H, Yasumoto K, Rouzaud F, Vieira WD, Hearing VJ. The Seiji memorial lecture: the melanosome: an ideal model to study cellular differentiation. *Pigment Cell Res* 2003;16:237–244. [PubMed: 12753396]
15. Slominski A, Wortsman J, Luger T, Paus R, Salomon S. Corticotropin releasing hormone and proopiomelanocortin involvement in the cutaneous response to stress. *Physiol Rev* 2000;80:979–1020. [PubMed: 10893429]
16. Lerner AB. The discovery of the melanotropins. A history of pituitary endocrinology. *Ann NY Acad Sci* 1993;680:1–12. [PubMed: 8512211]
17. Cone RD, Lu D, Koppula S, Vage DI, Klungland H, Boston B, Chen W, Orth DN, Pouton C, Kesterson RA. The melanocortin receptors: agonists, antagonists, and the hormonal control of pigmentation. *Recent Prog Horm Res* 1996;51:287–317. [PubMed: 8701084]
18. Eberle AN 1988 The melanotropins: chemistry, physiology and mechanism of action. New York: S. Karger Publishing
19. Geschwind II, Huseby RA, Nishioka R. The effect of melanocyte-stimulating hormone on coat color in the mouse. *Recent Prog Horm Res* 1972;28:91–130. [PubMed: 4631622]
20. Granholm NH, Van Amerongen AW. Effects of exogenous MSH on the transformation from phaeo- to eumelanogenesis within C57BL/6J-Ay/a hair-bulb melanocytes. *J Invest Dermatol* 1991;96:78–84. [PubMed: 1987299]
21. Hadley M 1996 Endocrinology. Englewood Cliffs, NJ: Prentice Hall
22. Tamate HB, Takeuchi T. Action of the e locus of mice in the response of phaeomelanin hair follicles to  $\alpha$ -melanocyte-stimulating hormone *in vitro*. *Science* 1984;224:1241–1242. [PubMed: 6328651]
23. Krude H, Biebermann H, Luck W, Horn R, Brabant G, Gruters A. Severe early-onset obesity, adrenal insufficiency and red hair pigmentation caused by POMC mutations in humans. *Nat Genet* 1998;19:155–157. [PubMed: 9620771]
24. Valverde P, Healy E, Jackson I, Rees JL, Thody AJ. Variants of the melanocyte-stimulating hormone receptor gene are associated with red hair and fair skin in humans. *Nat Genet* 1995;11:328–330. [PubMed: 7581459]
25. Robbins LS, Nadeau JH, Johnson KR, Kelly MA, Roselli-Rehffuss L, Baack E, Mountjoy KG, Cone RD. Pigmentation phenotypes of variant extension locus alleles result from point mutations that alter MSH receptor function. *Cell* 1993;72:827–834. [PubMed: 8458079]
26. Wolff GL. Regulation of yellow pigment formation in mice: a historical perspective. *Pigment Cell Res* 2003;16:2–15. [PubMed: 12519120]
27. Barsh G, Gunn T, He L, Schlossman S, Duke-Cohan J. Biochemical and genetic studies of pigment-type switching. *Pigment Cell Res* 2000;13(Suppl 8):48–53. [PubMed: 11041357]
28. Barsh GS, Ollmann MM, Wilson BD, Miller KA, Gunn TM. Molecular pharmacology of Agouti protein *in vitro* and *in vivo*. *Ann NY Acad Sci* 1999;885:143–152. [PubMed: 10816647]
29. Graham A, Wakamatsu K, Hunt G, Ito S, Thody AJ. Agouti protein inhibits the production of eumelanin and phaeomelanin in the presence and absence of  $\alpha$ -melanocyte stimulating hormone. *Pigment Cell Res* 1997;10:298–303. [PubMed: 9359625]
30. Siegrist W, Drozd R, Cotti R, Willard DH, Wilkison WO, Eberle AN. Interactions of  $\alpha$ -melanotropin and agouti on B16 melanoma cells: evidence for inverse agonism of agouti. *J Recept Signal Transduct Res* 1997;17:75–98. [PubMed: 9029482]
31. Rouzaud F, Annereau JP, Valencia JC, Costin GE, Hearing VJ. Regulation of melanocortin 1 receptor expression at the mRNA and protein levels by its natural agonist and antagonist. *FASEB J* 2003;17:2154–2156. [PubMed: 14500544]
32. Smith AI, Funder JW. Proopiomelanocortin processing in the pituitary, central nervous system, and peripheral tissues. *Endocr Rev* 1988;9:159–179. [PubMed: 3286233]
33. Autelitano DJ, Lundblad JR, Blum M, Roberts JL. Hormonal regulation of POMC gene expression. *Ann Rev Physiol* 1989;51:715–726. [PubMed: 2653201]
34. Yaswen L, Diehl N, Brennan MB, Hochgeschwender U. Obesity in the mouse model of proopiomelanocortin deficiency responds to peripheral melanocortin. *Nat Med* 1999;5:1066–1070. [PubMed: 10470087]

35. Challis BG, Coll AP, Yeo GS, Pinnock SB, Dickson SL, Thresher RR, Dixon J, Zahn D, Rochford JJ, White A, Oliver RL, Millington G, Aparicio SA, Colledge WH, Russ AP, Carlton MB, O'Rahilly S. Mice lacking pro-opiomelanocortin are sensitive to high-fat feeding but respond normally to the acute anorectic effects of peptide-YY(3–36). *Proc Natl Acad Sci USA* 2004;101:4695–4700. [PubMed: 15070780]
36. Smart JL, Low MJ. Lack of proopiomelanocortin peptides results in obesity and defective adrenal function but normal melanocyte pigmentation in the murine C57BL/6 genetic background. *Ann NY Acad Sci* 2003;994:202–210. [PubMed: 12851317]
37. Ermak G, Slominski A. Production of POMC, CRH-, ACTH- and  $\alpha$ -MSH-receptor mRNA and expression of tyrosinase gene in relation to hair cycle and dexamethasone treatment in the C57BL/6 mouse skin. *J Invest Dermatol* 1997;108:160–167. [PubMed: 9008228]
38. Slominski A, Paus R. Melanogenesis is coupled to murine anagen: toward new concepts for the role of melanocytes and the regulation of melanogenesis in hair growth. *J Invest Dermatol* 1993;101:90S–97S. [PubMed: 8326158]
39. Ito S, Fujita K. Microanalysis of eumelanin and pheomelanin in hair and melanomas by chemical degradation and liquid chromatography. *Anal Biochem* 1985;144:527–536. [PubMed: 3993914]
40. Kappenman KE, Dvoracek MA, Harvison GA, Fuller BB, Granholm NH. Tyrosinase abundance and activity in murine hairbulb melanocytes of agouti mutants (C57BL/6J-a/a, Ay/a, and AwJ/AwJ). *Pigment Cell Res Suppl* 1992;2:79–83.
41. Plonka PM, Slominski AT, Pajak S, Urbanska K. Transplantable melanomas in gerbils (*Meriones unguiculatus*). II: melanogenesis. *Exp Dermatol* 2003;12:356–364. [PubMed: 12930290]
42. Felix C, Hyde J, Sarna T, Sealy R. Interaction of melanins with metal ions. Electron spin resonance evidence for chelate complexes of metal ions with free radicals. *J Am Chem Soc* 1978;100:3922–3926.
43. Deibel R, Chedekel M. Biosynthetic and structural studies on pheomelanin. *J Am Chem Soc* 1982;104:7306–7309.
44. Pisarchik A, Slominski A. Alternative splicing of CRH-R1 receptors in human and mouse skin: identification of new variants and their differential expression. *FASEB J* 2001;15:2754–2756. [PubMed: 11606483]
45. Sealy RC, Hyde JS, Felix CC, Menon IA, Prota G. Eumelanins and pheomelanins: characterization by electron spin resonance spectroscopy. *Science* 1982;217:545–547. [PubMed: 6283638]
46. Sealy RC, Hyde JS, Felix CC, Menon IA, Prota G, Swartz HM, Persad S, Haberman HF. Novel free radicals in synthetic and natural pheomelanins: distinction between dopa melanins and cysteinyl-dopa melanins by ESR spectroscopy. *Proc Natl Acad Sci USA* 1982;79:2885–2889. [PubMed: 6283550]
47. Vsevolodov EB, Ito S, Wakamatsu K, Kuchina II, Latypov IF. Comparative analysis of hair melanins by chemical and electron spin resonance methods. *Pigment Cell Res* 1991;4:30–34. [PubMed: 1656423]
48. Okazaki M, Kuwata K, Miki Y, Shiga S, Shiga T. Electron spin relaxation of synthetic melanin and melanin-containing human tissues as studied by electron spin echo and electron spin resonance. *Arch Biochem Biophys* 1985;242:197–205. [PubMed: 2996430]
49. Busca R, Ballotti R. Cyclic AMP a key messenger in the regulation of skin pigmentation. *Pigment Cell Res* 2000;13:60–69. [PubMed: 10841026]
50. Oyehaug L, Plahte E, Vage DI, Omholt SW. The regulatory basis of melanogenic switching. *J Theor Biol* 2002;215:449–468. [PubMed: 12069489]
51. Slominski A, Tobin DJ, Shibahara S, Wortsman J. Melanin pigmentation in mammalian skin and its hormonal regulation. *Physiol Rev* 2004;84:1155–1228. [PubMed: 15383650]
52. Holst B, Elling CE, Schwartz TW. Metal ion-mediated agonism and agonist enhancement in melanocortin MC1 and MC4 receptors. *J Biol Chem* 2002;277:47662–47670. [PubMed: 12244039]
53. Kameyama K, Montague PM, Hearing VJ. Expression of melanocyte stimulating hormone receptors correlates with mammalian pigmentation, and can be modulated by interferons. *J Cell Physiol* 1988;137:35–44. [PubMed: 2459141]
54. Mundy NI, Badcock NS, Hart T, Scribner K, Janssen K, Nadeau NJ. Conserved genetic basis of a quantitative plumage trait involved in mate choice. *Science* 2004;303:1870–1873. [PubMed: 15031505]

55. Pawelek JM, Chakraborty AK, Osber MP, Orlow SJ, Min KK, Rosenzweig KE, Bologna JL. Molecular cascades in UV-induced melanogenesis: a central role for melanotropins? *Pigment Cell Res* 1992;5:348–356. [PubMed: 1292019]
56. Chluba-de Tapia J, Bagutti C, Cotti R, Eberle AN. Induction of constitutive melanogenesis in amelanotic mouse melanoma cells by transfection of the human melanocortin-1 receptor gene. *J Cell Sci* 1996;109:2023–2030. [PubMed: 8856498]
57. Sanchez-Mas J, Hahmann C, Gerritsen I, Garcia-Borrón JC, Jimenez-Cervantes C. Agonist-independent, high constitutive activity of the human melanocortin 1 receptor. *Pigment Cell Res* 2004;17:386–395. [PubMed: 15250941]
58. Parnot C, Miserey-Lenkei S, Bardin S, Corvol P, Clauser E. Lessons from constitutively active mutants of G protein-coupled receptors. *Trends Endocrinol Metab* 2002;13:336–343. [PubMed: 12217490]
59. Seifert R, Wenzel-Seifert K. Constitutive activity of G-protein-coupled receptors: cause of disease and common property of wild-type receptors. *Naunyn Schmiedebergs Arch Pharmacol* 2002;366:381–416. [PubMed: 12382069]
60. Nijenhuis WA, Oosterom J, Adan RA. AgRP(83–132) acts as an inverse agonist on the human-melanocortin-4 receptor. *Mol Endocrinol* 2001;15:164–171. [PubMed: 11145747]
61. Nie J, Lewis DL. Structural domains of the CB1 cannabinoid receptor that contribute to constitutive activity and G-protein sequestration. *J Neurosci* 2001;21:8758–8764. [PubMed: 11698587]
62. Rhee MH, Kim SK. SR144528 as inverse agonist of CB2 cannabinoid receptor. *J Vet Sci* 2002;3:179–184. [PubMed: 12514329]
63. Miura S, Saku K, Karnik SS. Molecular analysis of the structure and function of the angiotensin II type 1 receptor. *Hypertens Res* 2003;26:937–943. [PubMed: 14717335]
64. Audinot V, Newman-Tancredi A, Millan MJ. Constitutive activity at serotonin 5-HT(1D) receptors: detection by homologous GTPγS versus [(35)S]-GTPγS binding isotherms. *Neuropharmacology* 2001;40:57–64. [PubMed: 11077071]
65. Teitler M, Herrick-Davis K, Purohit A. Constitutive activity of G-protein coupled receptors: emphasis on serotonin receptors. *Curr Top Med Chem* 2002;2:529–538. [PubMed: 12052192]
66. Brillet K, Kieffer BL, Massotte D. Enhanced spontaneous activity of the mu opioid receptor by cysteine mutations: characterization of a tool for inverse agonist screening. *BMC Pharmacol* 2003;3:14. [PubMed: 14641935]
67. Rodien P, Ho SC, Vlaeminck V, Vassart G, Costagliola S. Activating mutations of TSH receptor. *Ann Endocrinol (Paris)* 2003;64:12–16. [PubMed: 12707626]
68. Shenker A. Activating mutations of the lutropin choriogonadotropin receptor in precocious puberty. *Receptors Channels* 2002;8:3–18. [PubMed: 12408104]
69. Schioth HB, Prusis P, Muceniece R, Mutulis F, Mutule I, Wikberg JE. Thyrotropin releasing hormone (TRH) selectively binds and activates the melanocortin 1 receptor. *Peptides* 1999;20:395–400. [PubMed: 10447100]
70. Slominski A, Wortsman J, Kohn L, Ain KB, Venkataraman GM, Pisarchik A, Chung JH, Giuliani C, Thornton M, Slugoeki G, Tobin DJ. Expression of hypothalamic-pituitary-thyroid axis-related genes in the human skin. *J Invest Dermatol* 2002;119:1449–1455. [PubMed: 12485453]

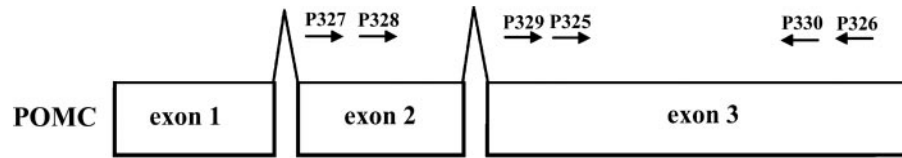


**Fig. 1.** Exon location of primers used to amplify mouse *Pomc* cDNA from skin. Primer sequences are provided in Table 1.

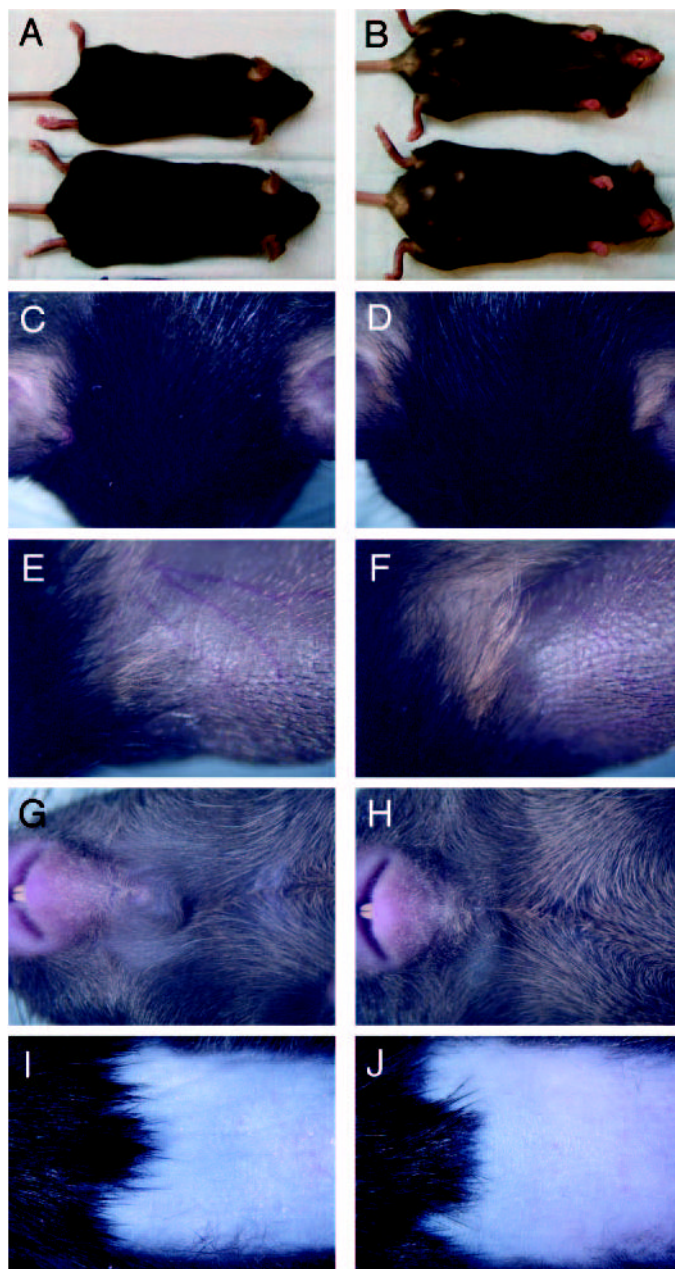


**Fig. 2.** Pigmentary phenotype of experimental mice. Dorsal (A) and ventral (B) views of 3-month-old sibling female *Pomc*<sup>+/+</sup> (upper) and *Pomc*<sup>-/-</sup> (lower) mice. Detailed views of the head (C and D), dorsal surface of ears (E and F), and ventral surface of neck (G and H) of 9-month-old sibling male *Pomc*<sup>+/+</sup> (C, E, and G) and *Pomc*<sup>-/-</sup> (D, F, and H) mice. Telogen hairs and adjacent anagen V skin (7 d after depilation) with regrowing hairs on the back of 9-month-old sibling male *Pomc*<sup>+/+</sup> (I) and *Pomc*<sup>-/-</sup> (J) mice.

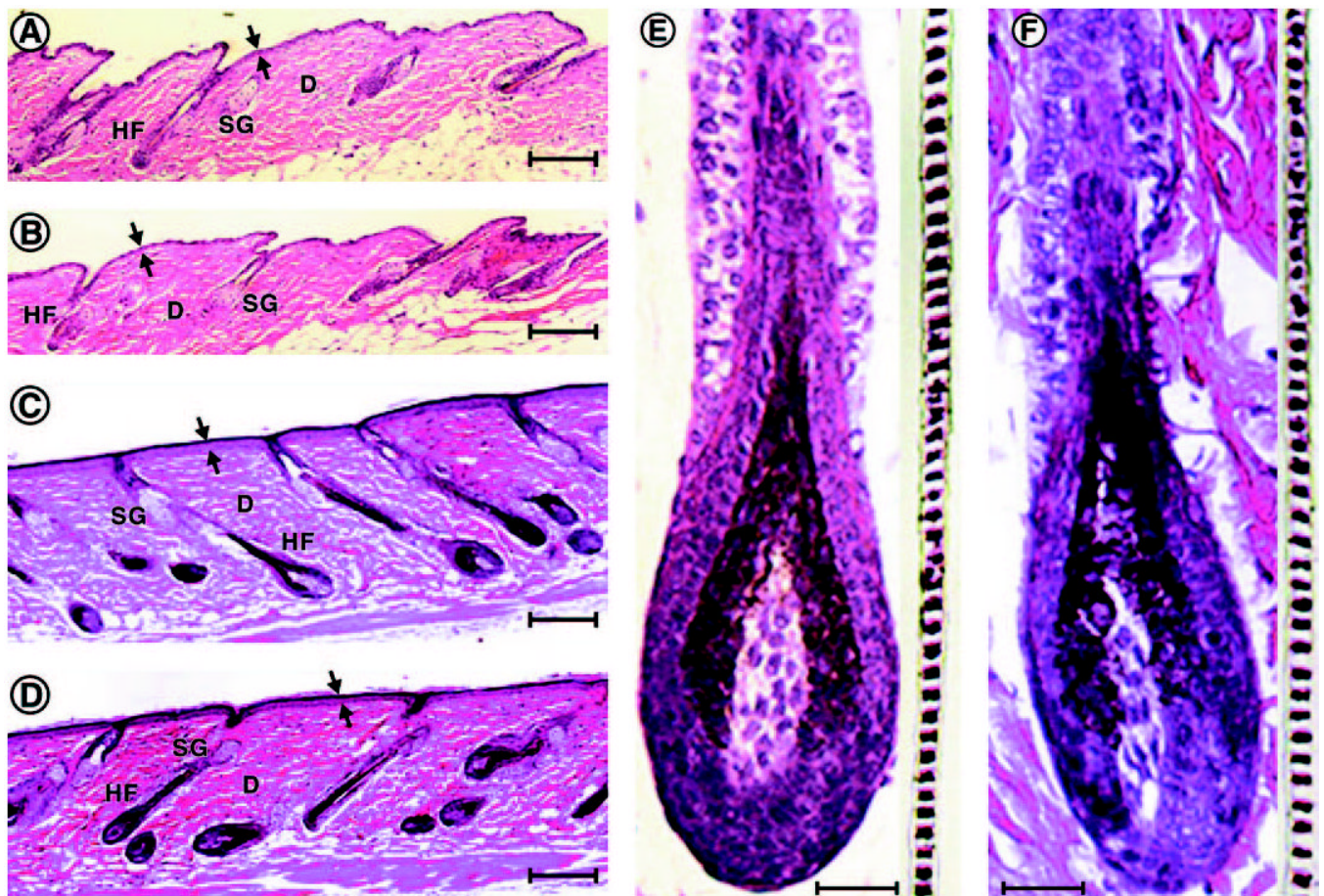


**Fig. 3.** Histology of the skin and hair follicles from experimental mice. The skin architecture and morphology of adnexal structures are similar in *Pomc*<sup>-/-</sup> (A, C, and E) and *Pomc*<sup>+/+</sup> (B, D, and F) mice. A and B, Skin with hair follicles at telogen phase. C and D, Skin with hair follicles at anagen V phase of hair growth. E and F, Detailed structures of anagen hair follicles (*left*) and hair shafts (*insets, right*) for *Pomc*<sup>-/-</sup> (E) and *Pomc*<sup>+/+</sup> (F) mice. *Two arrows*, epidermis; D, dermis; SG, sebaceous gland; HF, hair follicle. *Bar* (A–D), 160  $\mu$ m; (E and F), 40  $\mu$ m.

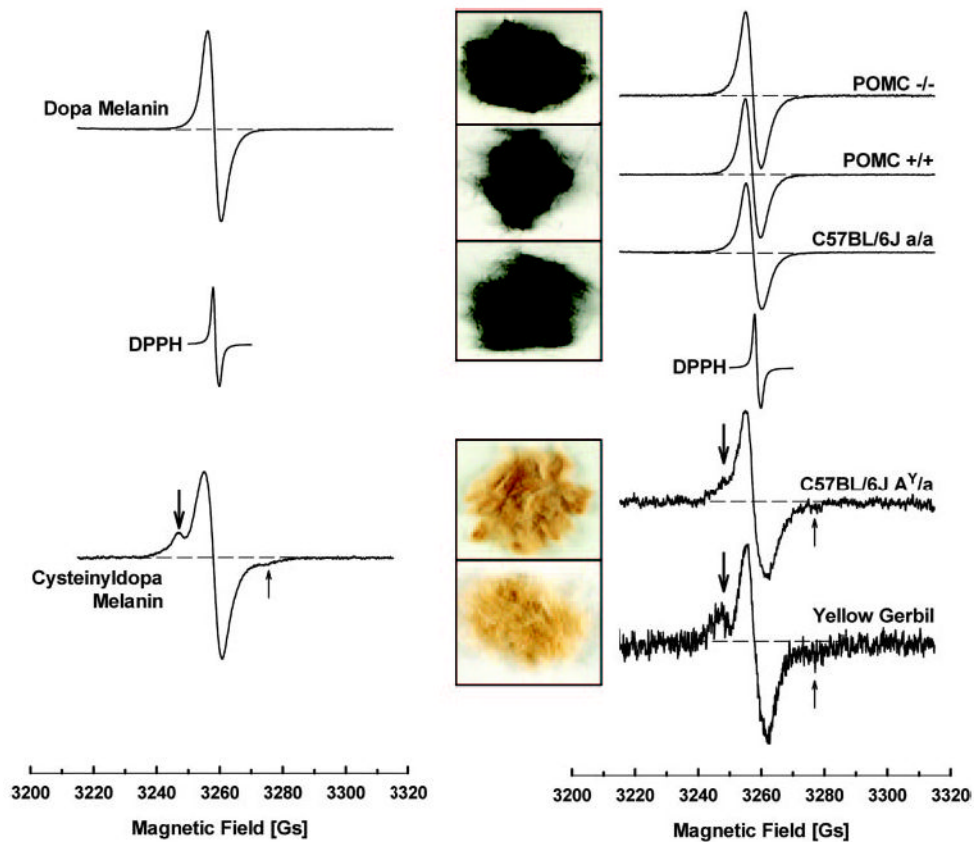


**Fig. 4.** Typical EPR spectra of synthetic (powder samples of 8.1 mg) and natural materials (dry fur samples of 20 mg) containing various contributions of pheomelanin. *Left panel*, Dopa melanin, a synthetic eumelanin-like pigment with a singlet, slightly asymmetric line; cysteinyldopa, the synthetic counterpart of pheomelanin with a characteristic  $^{14}\text{N}$  hyperfine splitting (*arrows*, the low-field line, *thick arrow*, are better pronounced than the high-field line, *thin arrow*). *Right panel*, Characteristic hyperfine splitting (*arrows*) was present only in the EPR spectra of yellow fur from  $A^y/a$  mice and yellow gerbils and absent in all the homogeneously black fur from  $Pomc^{-/-}$ ,  $Pomc^{+/+}$ , and standard C57BL/6J mice. *Insert*, Macrophotos of fur samples corresponding to the spectra on the right. DPPH, Position of free radical signal of DPPH. Parameters of assay, modulation amplitude 2 Gs; microwave power 1 mW; received gains of 12,500 (dopa melanin), 62,000 (cysteinyldopa melanin), 40,000 ( $Pomc^{-/-}$ ), 25,000 ( $Pomc^{+/+}$  and C57BL/6J  $a/a$ ), 800,000 (C57BL/6J  $A^y/a$ ), and 1 million (yellow gerbil); see also *Materials and Methods*.

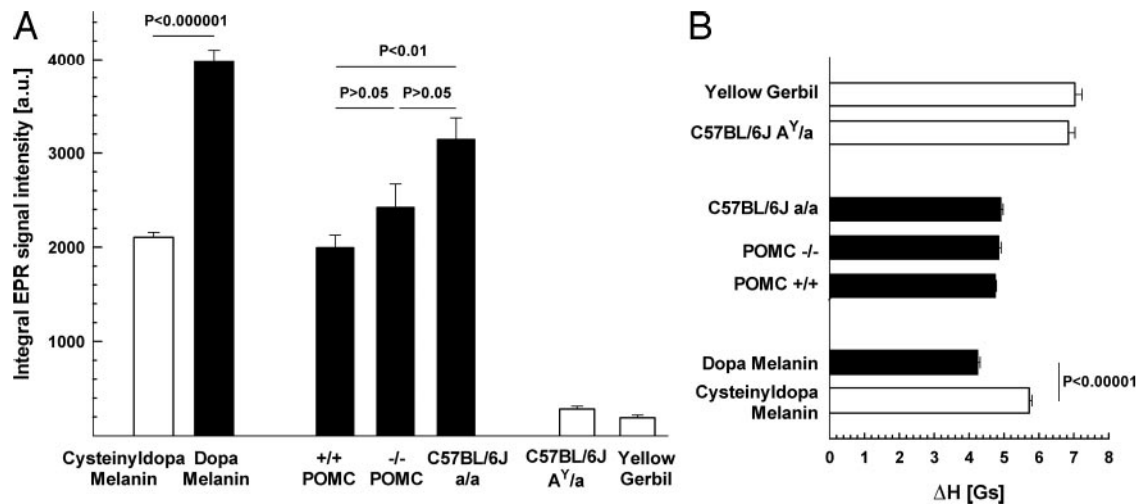


**Fig. 5.**

Quantitative analysis of the EPR measurements. A, Integral intensities of the EPR signals of analyzed materials. B, Peak-to-peak line widths of the EPR signals. All the bars represent means  $\pm$  sem of five independent samples (except *Pomc*<sup>-/-</sup> and yellow gerbil, n = 16 and 6 samples, respectively) of powdered substance (8.1 mg, synthetic melanins) or dry fur (20 mg). Parameters of assay of the integral signal intensities: microwave power, 1 mW; modulation amplitude, 5 Gs; gain, 12,500; parameters of assay of the signal line widths: microwave power, 1 mW; modulation amplitude, 0.5 Gs; see also *Materials and Methods*.

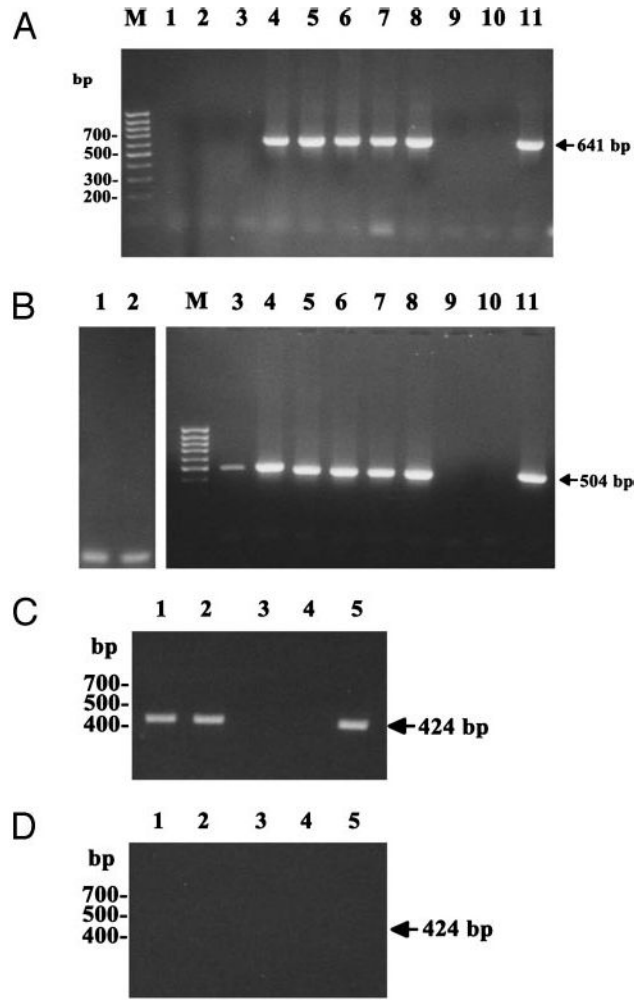


**Fig. 6.** Amplification of mouse *Pomc* gene products by nested RT-PCR. Exons 2 and 3 were amplified from cDNA with sets of primer pairs P327/P326 and P328/P330 (A) or P328/P326 and P329/P330 (B). Lane 1, Mouse skin *Pomc*<sup>-/-</sup> (total RNA); lane 2, mouse skin *Pomc*<sup>-/-</sup> (mRNA); lane 3, mouse skin *Pomc*<sup>+/-</sup> (total RNA); lane 4, mouse skin *Pomc*<sup>+/-</sup> (mRNA); lane 5, anagen mouse skin *Pomc*<sup>+/+</sup> (mRNA); lane 6, telogen mouse skin *Pomc*<sup>+/+</sup> (mRNA); lane 7, anagen mouse skin *Pomc*<sup>+/+</sup> (mRNA); lane 8, telogen mouse skin *Pomc*<sup>+/+</sup> (mRNA); lane 9, anagen mouse skin *Pomc*<sup>-/-</sup> (mRNA); lane 10, telogen mouse skin *Pomc*<sup>-/-</sup> (mRNA); lane 11, telogen skin from the *Pomc* transgene rescue mouse (mRNA). Primer pairs P329/P326 and P325/P330 from exon 3 were used to amplify cDNA (C) or RNA (D) without prior RT (RT, negative control). Lane 1, Anagen skin *Pomc*<sup>+/+</sup> mRNA; lane 2, telogen skin *Pomc*<sup>+/+</sup> (mRNA); lane 3, anagen skin *Pomc*<sup>-/-</sup> (mRNA); lane 4, telogen skin *Pomc*<sup>-/-</sup> (mRNA); lane 5, telogen skin from the *Pomc* transgene rescue mouse (mRNA).

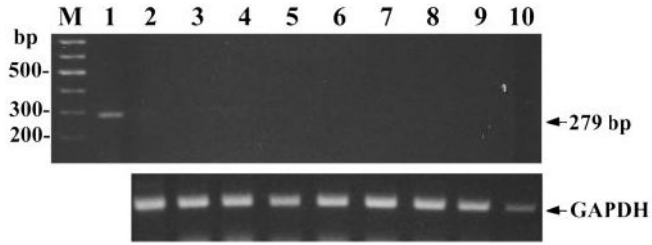


**Fig. 7.** Amplification of mouse *Pomc-ps1* pseudogene putative products by PCR. A, Amplification of *Pomc-ps1* pseudogene with primer pair P331/P332. B, Amplification of GAPDH (positive control). DNase-treated mRNA was used for RT in all samples with the exception of genomic DNA in lane 1. Lane 1, Genomic DNA; lane 2, mouse skin *Pomc*<sup>-/-</sup>; lane 3, mouse skin *Pomc*<sup>+/-</sup>; lane 4, mouse anagen skin *Pomc*<sup>+/+</sup>; lane 5, mouse telogen skin *Pomc*<sup>+/+</sup>; lane 6, mouse anagen skin *Pomc*<sup>+/+</sup>; lane 7, mouse telogen skin *Pomc*<sup>+/+</sup>; lane 8, mouse anagen skin *Pomc*<sup>-/-</sup>; lane 9, mouse telogen skin *Pomc*<sup>-/-</sup>; and lane 10, telogen skin from the *Pomc* transgene rescue mouse (mRNA).

TABLE 1

PCR amplification of the mouse *Pomc* gene and *Pomc-ps1* pseudogene

| Primer location | PCR1        |                         |                    | PCR2 (nested) |                         |                    |
|-----------------|-------------|-------------------------|--------------------|---------------|-------------------------|--------------------|
|                 | Primer name | Primer sequence         | Fragment size (bp) | Primer name   | Primer sequence         | Fragment size (bp) |
| Exons 2 and 3   | P327        | GTGGAAGATGCCCGAGATTCTG  | 746                | P328          | TCCTGCTTCAGACCTCCATAG   | 641                |
|                 | P326        | GGGGCCTTGGAATGAGAAGAC   |                    | P330          | GTTCTTGATGATGGCGTTCCTTG |                    |
|                 | P328        | TCCTGCTTCAGACCTCCATAG   |                    | P329          | CTGGCAACGGAGATGAACAG    |                    |
| Exons 2 and 3   | P326        | GGGGCCTTGGAATGAGAAGAC   | 693                | P330          | GTTCTTGATGATGGCGTTCCTTG | 504                |
|                 | P329        | CTGGCAACGGAGATGAACAG    |                    | P325          | CCCAGGAACAGCAGCAGTG     |                    |
| Exon 3          | P326        | GGGGCCTTGGAATGAGAAGAC   | 555                | P330          | GTTCTTGATGATGGCGTTCCTTG | 424                |
| Pseudogene      | P331        | ACTAATTTCAAGGAGGTTTTTCT | 279                |               |                         |                    |
|                 | P332        | GACGTGCTCCAAGCCATCAG    |                    |               |                         |                    |